ISSN-1996-918X

Pak. J. Anal. Environ. Chem. Vol. 16, No. 2 (2015) 38 – 47

EDTA Modified *Irvingia gabonensis*: An Efficient Bioresource Material for the Removal of Rhodamine B.

A. A. Inyinbor[*1,2], F. A. Adekola[2] and G. A. Olatunji[2]

[1]*Department of Physical Sciences, Landmark University, P.M.B 1001, Omu Aran, Nigeria.*

[2]*Department of Chemistry, University of Ilorin, P.M.B 1515, Ilorin, Nigeria.*

Received 21 April 2015, Revised 21 December 2015, Accepted 28 December 2015

Abstract

EDTA modified dika nut (*Irvingia gabonensis*) (EMDN) has been prepared, its physicochemical characteristics were determined and it was characterized using fourier transform infrared (FT-IR) spectroscopy and scanning electron microscopy (SEM). Brunauer–Emmett–Teller (BET) surface area of EMDN was obtained to be 8.092 m^2/g. Its efficiency in the uptake of Rhodamine B (RhB) from aqueous effluent was investigated and maximum adsorption was recorded at pH 6. Adsorption data fitted best into the Freundlich adsorption isotherm than the Langmuir, Temkin and Dubinin Raduskevich (D-R) models, the maximum monolayer adsorption capacity (q_{max}) obtained from the Langmuir equation was obtained to be 532.27 mg/g and the mean sorption energy (E) calculated from the D-R model was less than 8 $kJmol^{-1}$ suggesting that the adsorption process was physical in nature. Pseudo second order better described the kinetics of adsorption than the pseudo first order. Desorption percentage of RhB from EMDN surface was found to be low for all the desorbing eluents used and HCl has the highest desorption percentage of 17.75%.

Keyword: *Irvingia gabonensis*; Rhodamine B; Adsorption; SEM; FTIR.

Introduction

Textile industries are in the forefront in the use of dye and generate large volume of effluent in their operations [1]. The release of these effluents into the aquatic environment disrupts the penetration of sunlight and hinders dissolved oxygen thus leading to the death of aquatic organism. These dyes are known to be carcinogenic thus causing serious threat to human [2, 3]. Rhodamine B, a highly soluble xanthene dye has found great use in various dye utilizing industry because of their easy wet fastness. Due to their high solubility, molecules of this carcinogenic dye accompany the wastewater of such industries and subsequently enter into the environment via the discharge of such wastewaters [4, 5, 6]. The maximum concentration of Rhodamine B in wastewater has been fixed at 5 mg/L and tolerance limit for ingestion is 0.75 mg per day [7].Therefore, effluents containing this hazardous dye must be effectively treated before their discharge into the environment.

Adsorption using activated carbon due to its simplicity of operation and ability to remove low concentration of pollutants is a preferred option for effluents treatment compared with other conventional methods. However, materials used for the production of activated carbon are expensive; hence, there is a great need to develop alternative adsorbents [8,9]. Other adsorbents viz naturally occurring materials such as clay, industrial waste, synthesized nanomaterials and agricultural waste are currently been used as alternative adsorbents.

Biomass such as agricultural waste which composed basically of cellulose have been well investigated for their efficiency to remove

*Corresponding Author Email: fadekola@unilorin.edu.ng

toxicants such as dyes and heavy metals [2, 8, 10, 11, 12, 13, 14]. However, surface modification or functionalization of raw biomass, which introduces functional groups with unique binding characteristics enhances adsorption capacity of biomaterials thus resulting into adsorbents with superior adsorption capacity [15]. The efficiency of modified/functionalized biomass in the uptake of various toxicants has been previously investigated and reported [16, 17, 18].

Irvingia gabonensis (sweet bush mango also known as Dika fruit) is an agricultural product common in the South western Nigeria. It is a drupe with a thin epicarp, a soft fleshy thick mesocarp and a hard endocarp encasing a soft dicotyledonous kernel. Sweet bush mango in all its parts serves as food for human with the exception of its endocarp; the mesocarp and the epicarp can be eaten fresh while the cotyledon encased in the endocarp serves as soup recipe. The endocarp which is a lignocellulosic material however is an agricultural waste. This study aims at preparing an effective low cost adsorbent *via* surface modification using EDTA as chelating agent, characterization of the prepared adsorbent and its application for the uptake of a toxic dye (Rhodamine B).

Materials and Methods

All reagents used were of analytical grade and were used without further purifications. Deionized water was used throughout the experimental work. Endocarps of *Irvingia gabonensis* were collected from farmers in Omu Aran, Kwara State of Nigeria; it was thoroughly washed to remove dirts and dried in an oven operated at 105 ^{o}C overnight. It was then pulverized and screened into a particle size of 150-250 µm.

Modification with EDTA

The EDTA modification was done following the method reported by Ahmad et al 2009 [19], 0.1 M of EDTA was prepared by dissolving 29.225 g of EDTA in 1 dm^3 of deionized water, few pellets of NaOH was used to enhance the dissolution of the EDTA. Biomaterial and EDTA solution were mixed in ratio 1 to 10 and the mixture was agitated at room temperature for 24 hours. It was filtered, washed to neutrality and then dried in an oven operated at 105 ^{o}C. The prepared adsorbent (EMDN) was stored in an air tight container.

Characterization of EMDN

The topography and the elemental composition of EDTA modified dika nut (EMDN) was studied using a FEIESEM quanta 200 for SEM and EDX. Various functional groups present in EMDN were analyzed using a Bruker ALPHA FT-IR spectrophotometer. The BET surface area was obtained using a micrometric tristar II surface area and porosity analyzer while other physicochemical characterization such bulk density, pH point of zero charge (pHpzc), moisture content and ash content were also carried out.

Adsorbate used

RhB dye was supplied by BDH, a stock solution of RhB (1000 mg/L) was prepared; and serial dilution was made to obtain other lower concentrations required.

Batch adsorption studies

Batch adsorption studies with respect to initial pH, initial dye concentration, contact time, adsorbent dosage and temperature were carried out. Adsorption processes were performed by agitating a given dose of the adsorbent (1 g/L for initial pH, initial dye concentration and contact time and temperature effects studies) with 100 mL of RhB solution of desired concentration in different 250 cm^3 flasks in a temperature controlled water bath shaker operated at 27 ^{o}C for initial pH, initial dye concentration, contact time and adsorbent dosage studies. A shaking speed of 130 rpm was maintained throughout the experiment to achieve equilibrium. Desired pH was obtained by adjusting the pH with HCl or NaOH (0.1M). Samples were withdrawn at different time intervals, centrifuged and the supernatant was analyzed for change in dye concentration using a Beckman Coulter Du 730 UV–visible spectrophotometer operated at RhB λ_{max} (554 nm). The quantity of dye adsorbed at a given time q_t (mg/g) and percentage dye removed were

calculated according to equation 1 and 2 respectively.

$$q_t = \frac{(C_i - C_t) \times V}{M} \quad (1)$$

$$\% Removal = \frac{(C_i - C_t) \times V}{C_i} \times 100 \quad (2)$$

Where C_i and C_t are concentrations of RhB in solution at initial and at time t, V is the volume in liter and M is the weight of the adsorbent in g.

Mathematical modeling

Isotherm studies

The Langmuir, Freundlich, Temkin and Dubinin Radishkevich (D-R) isotherms were employed to analyze the adsorption equilibrium data.

Langmuir isotherm model

The Langmuir isotherm [20] assumes a monolayer adsorption with uptake of adsorbates to a uniform surface. It is expressed by the mathematical equation 3;

$$\frac{C_e}{q_e} = \frac{C_e}{q_{max}} + \frac{1}{q_{max} K_L} \quad (3)$$

Where C_e is the concentration of adsorbate in the solution at equilibrium (m/L), q_e is the equilibrium concentration of adsorbate on the adsorbent (mg/g), q_{max} is the maximum monolayer adsorption capacity of adsorbent (mg/g) and K_L is the Langmuir adsorption constant (L/mg). The plot of C_e/q_e versus C_e is expected to give a straight line with a slope $1/q_o$ and an intercept of $1/q_o K_L$. Dimensionless parameter (R_L) which can be obtained by the mathematical equation 4 confirms the favorability of the adsorption process,

$$R_L = \frac{1}{(1 + K_L C_o)} \quad (4)$$

Freundlich Isotherm model

The Freundlich isotherm [21] describes multilayer adsorption and is expressed mathematically as;

$$\log q_e = \frac{1}{n} \log C_e + \log K_f \quad (5)$$

Where q_e is the quantity of RhB dye on the adsorbent at equilibrium (mg/g), C_e is the equilibrium concentration of the adsorbate (mg/L); K_f and n are constants incorporating the factors affecting the adsorption capacity and the degree of non-linearity between the solute concentration in the solution and the amount adsorbed at equilibrium respectively. The Plots of log q_e against log C_e gives a linear graphs and parameters K_f and n can be obtained from the slopes and intercepts of the graph respectively.

Temkin isotherm models

The Temkin isotherm expressed by the equation 6 contains a factor that takes into account the adsorbent-adsorbate interactions [22].

$$q_e = BlnA + BlnC_e \quad (6)$$

Where q_e is amount of adsorbate adsorbed at equilibrium (mg/g); C_e is equilibrium concentration of adsorbate (mg/L). B which is a constant related to the heat of adsorption and it is expressed by B = RT/b, b is the Temkin constant (J/mol), T is the absolute temperature (K), R is the gas constant (8.314 J/mol K), and A is the Temkin isotherm constant (L/ g). B and A can be calculated from the slopes (B) and intercepts (B ln A) of the plot of q_e vs. ln C_e.

Dubinin Radushkevich (D-R) Isotherm models

Dubinin Radushkevich (D-R) model is a more general model that does not assume a homogenous surface or constant adsorption potential, D-R model gives information about sorption mechanism, whether chemisorption or physisorption [23] and it is expressed by the mathematical equation;

$$\ln q_e = lnq_o - \beta\varepsilon^2 \quad (7)$$

Where q_e is the amount of RhB ions adsorbed per unit weight of adsorbent (mg/g), q_o is the maximum sorption capacity, b is the activity coefficient related to mean sorption energy E

(kJ/mol) and Ɛ is the Polanyi potential and it is expressed by equation 8;

$$\varepsilon = RT\ln\left(1 + \frac{1}{C_e}\right) \quad (8)$$

Where R is the gas constant (J/mol K) and T is the temperature (K). β (mol^2/Jol^2) and q_o can be obtained from the slope and the intercept of the plot of ln q_e vs ε^2 respectively.

Kinetics model

The kinetics data were analyzed using the pseudo-first-order, pseudo-second-order and the intraparticle diffusion models.

Pseudo first order model

The pseudo first-order kinetic model of Lagergren [24] is expressed by mathematic relation 9;

$$\ln(q_e - q_t) = \ln q_e - k_1 t \quad (9)$$

Where q_e and q_t are quantity absorbed at equilibrium and at time t respectively (mg/g), and k_1 is the rate constant for the pseudo-first-order sorption (min^{-1}). A plot of ln (q_e–q_t) against t at different concentrations should give linear graphs with negative slopes from which k_1 and calculated quantity adsorbed at equilibrium (q_{cal}) can be obtained.

Pseudo second order model

The pseudo-second-order kinetic model [25]. can be represented by the mathematical equation;

$$\frac{t}{q_t} = \frac{1}{k_2 q_{e^2}} + \frac{t}{q_e} \quad (10)$$

Where K_2 is the rate constant of the pseudo-second-order equation in g/mg min^{-1}, q_e is the maximum sorption capacity in mg/g and q_t (mg/g) is the amount of sorption at time t. A plot of t/qt against t gives linear graphs from which q_e and k_2 can be calculated from the slope and intercepts.

Validation of kinetics models

Chi square (X^2) and sum square of error (SSE) were used to validate the kinetics models;

$$X^2 = \sum_{i=1}^{n} \frac{(q_{exp} - q_{cal})2}{q_{cal}} \quad (11)$$

$$\Delta q_e\,(\%) = 100\sqrt{\Sigma\left[\frac{q_{e,exp} - q_{e,cal})/q_{e,exp}}{N-1}\right.} \quad (12)$$

Intraparticle diffusion model

The intraparticle diffusion model [26] expressed by the mathematical equation 13;

$$q_t = k_{diff} t^{1/2} + C \quad (13)$$

Where q_t (mg/g) is the amount of adsorbate adsorbed at time t and K_{diff} ($mg/gmin^{-1/2}$) is the rate constant for intraparticle diffusion. The value of C explains the thickness of the boundary layer, the larger the intercept the greater the boundary layer effect. A plot of q_t versus $t^{1/2}$ should give a linear graph if intraparticle diffusion is involved in the sorption process and if the plot passes through the origin then intraparticle diffusion is said to be the sole rate-limiting step.

Adsorption thermodynamic studies

Adsorption process as a function of temperature were investigated, thermodynamic parameters ΔG^o, ΔH^o and ΔS^o, which are important in determining the feasibility, spontaneity and the nature of adsorbate-adsorbent interactions were obtained using the mathematical relations 14 and 15;

$$lnK_o = \frac{\Delta S^\circ}{R} - \frac{\Delta H^\circ}{RT} \quad (14)$$

$$\Delta G^o = -RT\ln K_o \quad (15)$$

Where K_o is given as q_e/C_e, T is the temperature in Kelvin and R is the gas constant. A plot of $\ln K_o$ versus 1/T should give a linear plot and ΔH^o and ΔS^o can be calculated from the slope and intercept respectively.

Desorption Experiment

In order to investigate the leaching/desorption of RhB from EMDN, deionized water, 0.1M HCl and 0.1M CH_3COOH

were used as desorbing agents. 0.1g of fresh adsorbent was added to 100 mL of 100 mg/L RhB solution at pH 6 and shaken for 50 minutes. The RhB-loaded sorbents was separated by centrifugation and the residual RhB concentration were determined using spectrophotometer as earlier described. The RhB loaded adsorbent was washed gently with water to remove any unadsorbed dye and dried. The desorption process was carried out by mixing 100mL of each desorbing agents with the dried adsorbent and shaken for a predetermined time and the desorbed RhB was determined spectrophotometrically. The desorbing efficiency was then calculated using the mathematical relation below;

$$\text{Desorption efficiency (\%)} = \frac{q_{de}}{q_{ad}} \times 100 \qquad (16)$$

Where q_{de} is the quantity desorbed by each of the eluent and q_{ad} is the quantity adsorbed by the adsorbent during loading.

Results and Discussion

Characterization of adsorbent

Table 1 depicts the physicochemical characteristics of EMDN, the bulk density, ash content and moisture content were found to be low, low moisture content suggest that adsorbent is not diluted hence, additional weight of adsorbent is not required. The carbon content is found to be high which makes the adsorbent suitable for dye uptake [27].

Table 1. **Characteristics of EMDN.**

Parameters	Values EMDN
pH	3.43
pH_{pzc}	2.00
Bulk density (g cm^{-3})	0.33
Moisture content (%)	3.33
Ash content (%)	0.77
BET surface area (m^2 g^{-1})	8.09
Average pore diameter (nm)	110.50
%C	79.20
%O	20.08

The BET surface area is low, this is a characteristic of agricultural waste [28] FT-IR spectrum of EMDN (figure not shown) before dye adsorption shows strong adsorption bands at 1024 cm^{-1}, 1232 cm^{-1}, 1731 cm^{-1}, 2907 cm^{-1} and 3338 cm^{-1} their assignment is as listed in Table 2. There were shift in the adsorption band of EMDN after dye adsorption. This suggests that these functional groups participated in the adsorption of RhB [27].

Table 2. **FTIR spectral characteristics of EMDN before and after RhB adsorption.**

Assignment for IR peak	Before adsorption	Wave number (cm^{-1}) *After adsorption*	Differences
C-N stretching	1024	1023	-1
C-OH stretching	1232	1229	-3
C=O stretching	1731	1732	1
C-H stretching	2907	2911	4
O-H of alcohol	3338	3324	-14

Figure 1 shows the SEM analysis of EMDN, the surface of EMDN before dye adsorption was smooth and with numerous pores. However, the surface of EMDN after dye adsorption was observed to be rough and the pores earlier observed have been covered by the dye.

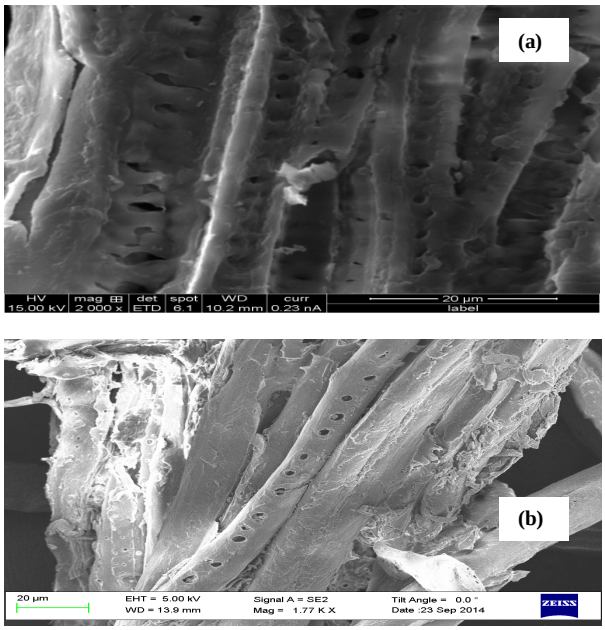

Figure 1. **SEM micrograph of EMDN (a) before dye adsorption (b) after dye adsorption**

Batch adsorption studies

Effects of pH on RhB uptake onto EMDN.

Fig. 2 depicts the effects of pH on RhB adsorption onto EMDN, adsorption percentage was observed to increase as the initial solution pH

increased and goes to equilibrium after pH 6. The PZC of the adsorbent was obtained to be 2 and above the PZC, the surface of the adsorbent is expected to be negative [29]. The attraction between the negative surface of the adsorbent and the cationic dye results into increase in the adsorption percentage as the pH increased. Subsequent studies were carried out at the optimum pH i.e pH of 6.

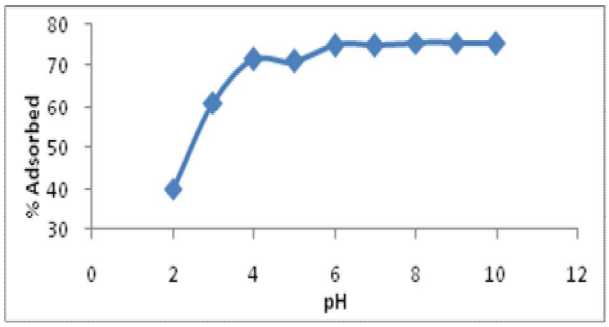

Figure 2. **Effects of pH on RhB uptake onto EMDN. Conditions: Adsorbent dose (1g/L), agitation speed (130 rpm), agitation time (60 minutes), Temperature (26°C), Adsorbate concentration (100 mg/L).**

Effects of adsorbent dosage on RhB uptake onto EMDN.

Percentage adsorption was observed to increase as the adsorbent dosage increased from 1 g/L to 3 g/L after which equilibrium was attained (Fig. 3). Increase in available adsorption sites created by the increase in adsorbent dosage resulted to increase in percentage adsorption [30]. However, agglomeration and adsorption site saturation may be responsible for the equilibrium attained after 3 g/L adsorbent dosage [31].

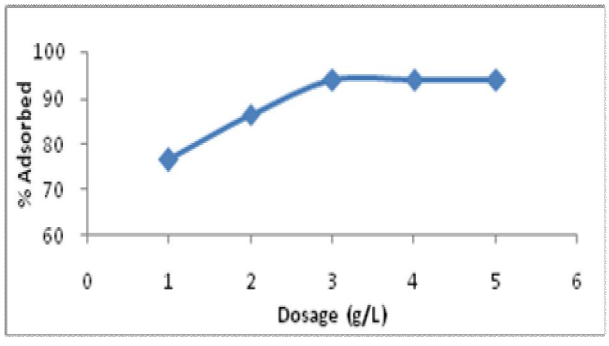

Figure 3. **Effects of adsorbent dosage on RhB uptake onto EMDN. Conditions: Initial concentration (100 mg/L), agitation speed (130 rpm), Temperature (26°C), pH (6)**

Effects of contact time and initial adsorbate concentration on RhB uptake onto EMDN.

Quantity adsorbed increased as the initial RhB concentration and contact time increased (Fig. 4), and equilibrium was attained between 40 and 60 minutes for all the initial dye concentrations considered. Quantities adsorbed at equilibrium were 40.29, 71.96, 150.33, 214.89, and 259.61 mg/g for initial RhB concentrations of 50, 100, 200, 300, and 400 mg/L, respectively. Higher initial concentration enhances adsorption process, initial concentration increases the driving force thus breaks mass transfer barriers between the adsorbate in solution and adsorbent [8].

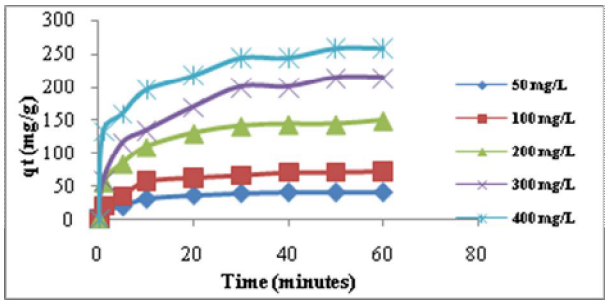

Figure 4. **Effects of contact time/initial adsorbate concentrations on RhB uptake onto EMDN Conditions: Adsorbent dose (1g/L), agitation speed (130 rpm), Temperature (26°C), pH (6)**

Effects of temperature on RhB uptake onto EMDN

Quantity adsorbed was observed to decrease rapidly as the temperature of the system increased (Fig. 5). Quantity adsorbed decreased from 70.56 mg/g to 18.25 mg/g as temperature increased from 26 °C to 60 °C. Increased solubility of dye may result into high affinity for solvent in which it was dissolved than for the adsorbent thus resulting into decrease in uptake of RhB as the temperature increased [30].

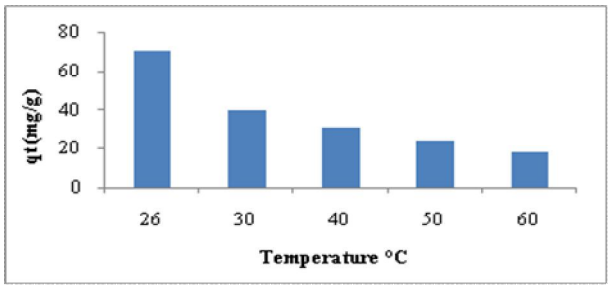

Figure 5. **Effects of temperature on the uptake of RhB onto EMDN. Conditions: Initial concentration (100 mg/L), agitation speed (130 rpm), adsorbent dosage (1 g/L), pH (6)**

Adsorption isotherm studies

The calculated isotherm parameters are listed in (Table 3). Comparing the R^2 values, the data was observed to fit best into the Freundlich adsorption isotherm suggesting that uptake of RhB was onto a non-uniform site. R^2 value for the Temkin and D-R isotherms were 0.9361 and 0.9810 respectively suggesting that some adsorbate-adsorbate interactions occurred during the uptake of RhB onto EMDN. The value of n was obtained to be greater than 1 suggesting that the adsorption process was favourable. The favourability of the adsorption process was further validated by the value of R_L calculated (0.0073). The E value obtained from the D-R model was less than 8 which suggests that the uptake of RhB onto EMDN was physical in nature. The maximum monolayer adsorption capacity (q_{max}) obtained from Langmuir equation was 526.32 mg/g and (Table 4) compares the maximum monolayer adsorption capacity of EMDN with that of other adsorbents available in the literatures, EMDN was found to be very effective thus have higher adsorption capacity.

Table 3. **Parameters of Langmuir, Freundlich, Temkin and D-R adsorption isotherm for the uptake of RhB onto EMDN.**

Isotherms	Constants	EMDN
Langmuir	q_{max} (mg/g)	526.32
	K_L (L.mg^{-1})	0.01
	R_L	0.26
	R^2	0.8193
Freundlich	K_F	7.17
	n	1.34
	R^2	0.9725
Temkin	B	86.62
	A (L/g)	0.13
	b (J/mol)	28.79
	R^2	0.9361
D-R	q_o (mg/g)	251.51
	β(mol^2.kJ^{-2})	0.17
	E (kJmol^{-1})	1.71
	R^2	0.9810

Table 4. **Comparison of adsorption capacity of RhB onto EMDN with various adsorbents.**

Adsorbent	q_{max} (mg/g)	Ref
Microwave treated nilotica leaf	24.39	[32]
Animal bone meal	62.11	[33]
Modified coir pith	14.90	[34]
Modified ternary waste	213.00	[35]
Treated fruit waste	34.48	[36]
Sugarcane baggase	51.50	[37]
Cedar Cone	4.55	[38]
Bakers' yeast	25.00	[39]
Modified Dika nut	526.32	This study

Adsorption kinetics studies

Table 5 compares the kinetic models used, R^2 value for the pseudo second order kinetics ranged between 0.9950 and 0.9982. High R^2 values, close agreement between q experimental and q calculated coupled with low values of X^2 and Δq_e in the case of pseudo second order kinetics suggests that this model well describes the uptake of RhB onto EMDN. A multilinear profile was obtained for the intraparticle diffusion model. Adsorption was in two stages, the first stage depicts adsorption process due to boundary layer diffusion while the second stage involves the intraparticle diffusion of adsorbate until equilibrium was attained. The plot of q_t versus square root of time (Fig. 6) did not pass through the origin, this further indicate that some degree of boundary layer diffusion also occurred during the uptake of RhB onto EMDN. Since the values of K_{1diff} are greater than the values of K_{2diff} across concentrations investigated (Table 5), this suggests that intraparticle diffusion mainly controlled the adsorption rate [40].

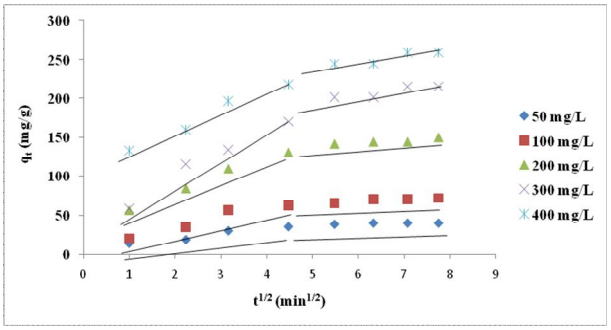

Figure 6. **Intraparticle diffussion plot of adsorption of RhB onto EMDN**

Table 5. **Comparison of Pseudo-first-order, Pseudo-second-order and intra particle diffusion kinetic model.**

Constants	EMDN				
	Initial Concentrations				
	50	***100***	***200***	***300***	***400***
$q_{e\ experimental}$ (mg/g)	40.29	71.96	150.33	214.89	259.61
	Pseudo first order				
$q_{e\ calculated}$ (mg/g)	22.68	46.52	79.03	197.35	169.02
K_1 X 10^{-3} (min^{-1})	7.33	7.61	6.11	8.88	8.49
R^2	0.9326	0.9561	0.9382	0.9036	0.8894
Δq_e (%)	0.11	0.08	0.13	0.01	0.08
X^2	13.67	13.91	64.33	1.56	48.55
	Pseudo second order				
$q_{e\ calculated}$ (mg/g)	43.29	76.92	156.25	232.56	270.27
K_2 X 10^{-3} ($gmg^{-1}min^{-1}$)	5.90	3.05	1.82	0.79	1.17
R^2	0.9969	0.9978	0.9982	0.9950	0.9969
Δq_e (%)	0.01	0.01	0.01	0.01	0.01
X^2	0.21	0.32	0.22	1.34	0.42
	Intra particle diffusion				
C_1 (mgg^{-1})	7.38	8.63	35.51	34.94	107.69
K_{1diff}($mgg^{-1}min^{-1/2}$)	6.52	12.86	21.96	31.25	25.46
R_1^2	0.9514	0.9355	0.9898	0.9706	0.9768
C_2 (mgg^{-1})	35.95	53.39	123.50	158.01	201.33
K_{2diff}($mgg^{-1}min^{-1/2}$)	0.59	2.45	3.28	7.48	7.67
R_2^2	0.6464	0.8184	0.8135	0.7948	0.7948

Thermodynamic studies

Thermodynamic parameters for the uptake of RhB onto EMDN are presented in Table 6. ΔH^o and ΔS^o were calculated from the slope and intercept of the Van't Hoff plot (Figure not shown). Negative enthalpy (ΔH^o) obtained for the uptake of RhB onto EMDN indicates that the adsorption process was exothermic in nature. The negative values of ΔS^o (Table 6) indicate decrease in the randomness at the solid-liquid interface during sorption of RhB onto EMDN. Adsorption process was feasible and spontaneous at ordinary room temperature thus a negative ΔG^o value was obtained (Table 6), however, at higher temperature, adsorption could not be well sustained. Increase in temperature may also have facilitated adsorbate-adsorbate interactions hence, the degree of quantity adsorbed at high temperature. Similar trend have been previously reported Using resin D301 as adsorbent [41].

Table 6. **Thermodynamic parameters for uptake of RhB onto EMDN.**

Adsorbent	ΔH^o (kJ/mol)	ΔS^o (J/mol/K)	ΔG^o (kJ/mol)				
			300	303	313	323	333
EMDN	-50.15	-164.60	-2.35	1.05	2.11	3.11	4.15

Desorption studies

The desorption efficiency of the eluents used was found to be generally low, it follows the order $HCl>CH_3COOH>H_2O$ with corresponding values of 17.78 %>13.3 % >8.87 %. It has been reported that large net adsorption energy can be established between large molecules and biosorbents due to several contact points; this in turn makes dye release from the surface of the adsorbent difficult [42].

Conclusion

The PZC of the adsorbent was obtained to be 2 hence adsorption increased as initial pH increased and goes to equilibrium after pH 6. Pseudo-second-order model better describe the kinetics of the adsorption process than the Pseudo first order kinetics model while a multilinear profile was obtained for the intraparticle diffusion studies. Freundlich adsorption isotherm best describe the adsorption equilibrium data thus adsorption was onto a non-uniform site. R^2 value for the Temkin adsorption isotherm was high suggesting some degree of adsorbate-adsorbate interactions. Adsorption energy obtained for D-R isotherm for the adsorption process was found to be less than 8 kJ mol^{-1} this suggests that the uptake of RhB onto EMDN was physical in nature. Desorption efficiency across eluents used was less than 25 %. About 95 % removal was recorded for optimum adsorbent dosage (3 g/L) from a 100 mg/L solution thus wastewater with RhB moderate pollution may be effectively treated with EMDN to attaining the allowable discharge limit.

Reference

1 F. N. Memon and S. Memon, *Sep. Sci. Technol.*, 50 (2015) 1135.

2 A.S. Sartape, A.M. Mandhare, V.V. Jadhav, P.D. Raut, M.A. Anuse and S.S. Kolekar, *Arab. J. Chem.* (2014), http://dx.doi.org/10.1016/j.arabjc.2013.12.019.

3 F. N. Memon, S. Memon, F. T. Minhas, C. R. *Chimie* 17(2014) 577.

4 M. El Haddad , R. Mamouni , N. Saffaj , and S. Lazar; *J. Saudi Chem. Soc.* (2012), http://dx.doi.org/10.1016/j.jscs.2012.08.005

5 K. Shen, M. A. Gondal, *J. Saudi Chem. Soc.* (2013), http://dx.doi.org/10.1016/j.jscs.2013.11.005

6 T. Santhi, A.L. Prasad, and S. Manonmani, *Arab. J. Chem.*, 7 (2014) 494.

7 Application note: Fluorescent tracer dyes. Available on http://www.turnerdesigns.com/t2/doc/appnotes/998-5104.pdf

8 B. H. Hameed, D. K. Mahmoud and A. L. Ahmad, *J. Haz. Mat.* 158 (2008) 65.

9 R. Jayaraj, M. Chandra, P. Martin Deva Prasath and T. K. Hidhayathullah *E-J. Chem.*, 8 (2011) 649.

10 U.J. Etim, S.A. Umoren , U.M. Eduok, *J. Saudi Chem. Soc.* (2012), http://dx.doi.org/10.1016/j.jscs.2012.09.014

11 M. M. Zuy, , Z. C. Mohana, F. D. Priscila, C. A. Fernanda, F. R. Ricardo and A. S. Adelir *J. Environ. Chem. Eng.* 2 (2014) 1731.

12 Z. K. George, K. L. Nikolaos, C. M. Athanassios *Chem. Eng. J.* 189– 190 (2012) 148.

13 O.S. Bello, and M.A. Ahmad, *Toxicol. Environ. Chem.*, 93 (2011) 1298–1308.

14 S. Noreen, H. N. Bhatti, S. Nausheen, S. Sadaf, and M. Ashfaq, *Indus. Crop. Prod.* 50 (2013) 5689.

15 Z. Wenxuan, L. Haijiang, K. Xiaowei, D. Lei, Y. Han, J. Ziwen, Y. Hu, L. Aimin, and C. Rongshi,; *Bioresource Technol.* 117 (2012) 40.

16 L. Zhou, J. Jin, Z. Liu, X. Liang and C. Shang; *J. Hazard. Mater.* 185 (2011) 1045.

17 T. Li, Y. Liu, Q. Peng, X. Hu, T. Liao, H. Wang and M. Ming Lu, *Chem. Eng. J.* 214 (2013) 189.

18 D. Gao, Q., Hu, H., Pan, J., Jiang, and P. Wang, *Bioresource Technol*. 193 (2015) 512.

19 D. Ahmad, D., Mukhtar-Ul-Hassan, H.N. Khalid, N. J., Khatoon and B. F. Hafza, *J. Sci. Res.*, 39 (2009) 1.

20 I. Langmuir, *J. Am. Chem. Soc*., 38 (1916) 2221.

21 H. M. F. Freundlich, *Z. Phys. Chem.*, 5 (1906) 3850.

22 M. I. Temkin, and V. Pyzhev, Kinetics of ammonia synthesis on promoted iron catalyst. *Acta Physiochim. USSR* 12 (1940) 327.

23 M. M. Dubinin and L. V. Radushkevich, *Proc. Acad. Sci. Phys. Chem. USSR*, 55 (1947) 331.

24 S. Lagergren and B.K. Svenska, *R. Swed. Acad. Sci. Doc, Band*, 24 (1898)1.

25 Y.S. Ho and G. McKay, *Proc. Biochem*, 1999, 34 (1999) 451.

26 W. J. Weber and J. C. Morris. *J. Sanity Eng. Div.*, 1963, 89 (1963) 31.

27 O. S. Bello, M. A., Ahmad and N. Ahmad, N.; *Chem. Ecol.*, 28 (2012) 153.

28 A. A. Inyinbor, F. A. Adekola and G. A., Olatunji, *S. Afr., J. of Chem*., 68 (2015) 115-125.

29 N. A. Alyoshina, A. V. Agafonov and E. V, Parfenyuk, *Mat. Sci. Eng. C* 40 (2014)164.

30 A. M. Aljeboree , A. N. Alshirifi and A. F. Alkaim, *Arab. J. Chem.* (2014), http://dx.doi.org/10.1016/j.arabjc.2014.01.020.

31 D. Angin, *Bioresource Technol*. (2014) http://dx.doi.org/10.1016/j.biortech.2014.02.100.

32 T. Santhi, A. L. Prasad and S. Manonmani, S., *Arab. J. Chem.*, 7 (2014) 494.

33 M. El Haddad, R. Mamouni, N. Saffaj and S. Lazar, *Global J. Human Soc. Sci. Geogr. Environ. Geo Sci.*, 12 (2012) 1.

34 M. V. Sureshkumar and C. Namasivayam, C. *Colloid. Surface. A,* 317 (2008) 277.

35 J. Anandkumar and B. Mandal, *J. Hazard. Mater.*, 186 (2011)1088.

36 P. Parimaladevi and V. Venkateswaran, *J. Appl. Technol. Environ. Sanit.*, 1 (2011) 285.

37 Z. Zhang, M. O. Ian, K.A. Geoff and O. S. D. William, *Indus. Crop. Prod.* 42 (2013) 41.

38 M. Zamouche and O. Hamdaoui, *Energy Procedia* 18 (2013) 1228.

39 J. Yu, B. Li, X. Sun, Y. Jun and R. Chi, *Biochemical Engineering Journal*; 45 (2009) 145.

40 O. S. Bello, M. Auta and O. B. Ayodele *Chemistry and Ecology*, 27 (2013) 58.

41 Chen, F., Zhou, C., Li, G., Peng, F., *Arabian Journal of Chemistry* (2012), http://dx.doi.org/10.1016/j.arabjc.2012.04.014

42 M. E. Fernandez, G. V. Nunell, P. R. Bonelli and A. L. Cukierman, *Bioresour. Technol.*; 101 (2010) 9500.